

Transition through triaxial shapes of the light samarium isotopes and the beta decay of $^{136,138,140}\text{Eu}$

B. D. Kern

University of Kentucky, Lexington, Kentucky 40506

R. L. Mlekodaj and G. A. Leander

UNISOR, Oak Ridge Associated Universities, Oak Ridge, Tennessee 37831

M. O. Kortelahti and E. F. Zganjar

Louisiana State University, Baton Rouge, Louisiana 70803

R. A. Braga, R. W. Fink, and C. P. Perez

School of Chemistry, Georgia Institute of Technology, Atlanta, Georgia 30332

W. Nazarewicz* and P. B. Semmes†

Joint Institute for Heavy-Ion Research, Oak Ridge, Tennessee 37831

(Received 11 May 1987)

Levels in $^{136,138,145}\text{Sm}$ were populated by the beta decay of Eu, following (HI,pxn) reactions and on-line mass separation. The beta decay of ^{136}Eu with a half-life of $3.9(\pm 0.5)$ s was observed for the first time. Members of the γ band were observed in all three daughter nuclei. Spectroscopic calculations were made using the triaxial rotor model, with all parameters derived microscopically from a Woods-Saxon deformed shell model. Other spectroscopic models were also considered. Comparison with the data supports the characterization of these nuclei in terms of a triaxial intrinsic shape.

I. INTRODUCTION

A transition from spherical to deformed shape in ^{62}Sm isotopes with $N < 82$ has long been predicted on the basis of elementary shell structure considerations,¹ and was borne out by recent measurements² of yrast level energies down to $N = 72$. The detailed nature of this shape transition is of interest in nuclear structure physics for comparison with the analogous shape transition at $N > 82$. The latter takes place abruptly as a function of N when $Z \approx 62$, between the spherical vibrator and prolate rotor regimes. Available evidence indicates that the transition at $N < 82$ is quite different. The onset of quadrupole deformation takes place more gradually² (although the details of this have not yet been fully charted, cf. Sec. IV below). Another prominent difference was predicted by a calculation of potential energy surfaces using the modified oscillator deformed shell model.³ All the experimentally accessible nuclear species with $50 < N < 82$ were found to be softer with respect to triaxial γ deformation than their $N > 82$ counterparts. In particular, the nucleus ^{138}Sm was found to have not only a small prolate-oblate energy difference but also a triaxial equilibrium shape. A similar result for this nucleus was obtained in a Hartree-Fock calculation with the Skyrme III force.⁴

In this paper we make the following contributions to the experimental and theoretical understanding of the $N < 82$ transitional Sm isotopes:

- (i) Level schemes for the $N = 74, 76,$ and 78 isotopes

of samarium are constructed from the γ rays following β decay of $^{136,138,140}\text{Eu}$. The β decay of ^{136}Eu was observed for the first time. A preliminary report on our study of ^{136}Eu decay was given in Ref. 5, and on ^{138}Eu decay in Ref. 6. A more extensive level scheme for ^{138}Sm , also from the β decay of ^{138}Eu , has been given by Charvet *et al.*⁷

- (ii) Potential-energy surfaces are calculated with yet another parametrization of the mean field, the "Warsaw" Woods-Saxon potential.⁸ Axial and triaxial rotor model spectra are derived from the equilibrium configurations and compared with the data.

- (iii) The experimental γ bands are also compared with predictions of the interacting boson model obtained from previously existing parameter sets.⁹⁻¹¹

II. EXPERIMENTAL PROCEDURES

The tandem accelerator at the Holifield Heavy Ion Research Facility provided beams of heavy ions that were used to produce radioactive Eu ions through (a) the $^{92}\text{Mo}(^{48}\text{Ti}, \text{pxn})$ reactions at 220 MeV and (b) the $^{112}\text{Sn}(^{28}\text{Si}, \text{pxn})$ reactions at 170 and 190 MeV; isotopically enriched targets of ^{92}Mo and ^{112}Sn were used. Ions recoiling from the target were introduced into a high-temperature ion source⁶ and passed through the UNISOR mass separator.¹² Also, in order to enhance the yields, a He-jet measurement was carried out without mass separation using reaction (b). In both experimental arrangements, radioactive ions were trans-

ported on a continuous plastic tape from a collection point to a γ -ray counting location that was situated between two Ge detectors. Data, recorded in the event mode on magnetic tapes, included pulse height for both γ -ray singles and γ - γ coincidence events, the time-to-analog converter pulse (TAC) for coincident events, and the time after the initiation of each counting interval. Additional experimental details have been given elsewhere.¹³⁻¹⁵

III. EXPERIMENTAL RESULTS

A. $^{136}\text{Eu} \rightarrow ^{136}\text{Sm}$

Previously, no observation of the β decay of ^{136}Eu had been accomplished. Our task of identification was aided by knowledge of the energies of the γ rays emitted in the ground-state yrast cascade in ^{136}Sm which has been reported by Lister *et al.*² The decay of ^{136}Eu to ^{136}Sm was studied with the magnetic separator and reaction (a) with collection and counting times of 8 s, in order to identify the mass, element, and principal γ rays. Then in order to enhance the yields, the He-jet technique and reaction (b) were used, with collection and counting times of 10 s.

The assignment of the yrast cascade² to $A = 136$ is confirmed by the magnetic separator results in which the 536-433-256-keV γ ray cascade was obtained. We have measured the half-life of the β decay of ^{136}Eu for the first time; a typical decay curve with half-life of 3.9 ± 0.5 s is shown in Fig. 1. The partial level scheme of the daughter ^{136}Sm (Fig. 2) was constructed with use of the singles spectra, the γ - γ gated spectra, and the relative intensities of the γ rays. The intensities of the 256.0, 432.9, and 535.5 keV γ rays have been corrected for $E2$ internal conversion. The sparse data restricted the making of definite assignments to only these few levels. The tentative identification of the 714.3 and 1172.3-keV levels as the 2^+ and 3^+ of the quasigamma band is consistent with the systematics of this region.

B. $^{138}\text{Eu} \rightarrow ^{138}\text{Sm}$

At approximately the time of the completion of this work, there appeared several publications on ^{138}Sm . To-

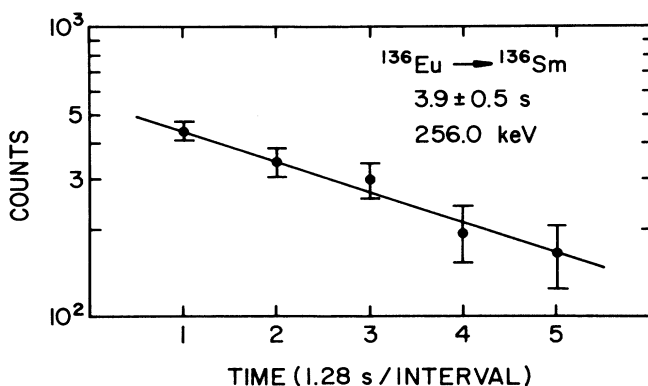


FIG. 1. The decay of the 256.0-keV γ ray due to the beta decay of ^{136}Eu .

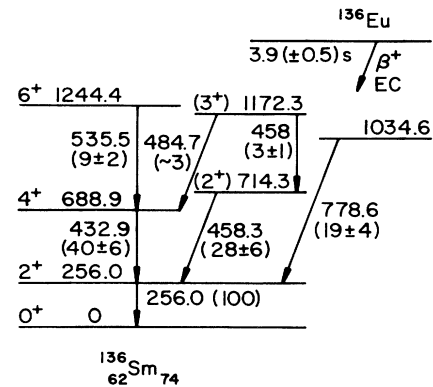


FIG. 2. Partial level diagram for ^{136}Sm . The energies are in keV and the relative intensities are given in the parentheses.

gether they give a consistent picture of the low-lying yrast cascade levels^{2,11,16} and the γ -band levels⁷ of ^{138}Sm . In our work with magnetically separated ^{138}Eu ions, the γ rays of the $8^+ - 6^+ - 4^+ - 2^+ - 0^+$ yrast cascade were found to decay with a half-life of 12 ± 1 s; this result is in agreement with the concurrent report of Charvet *et al.*⁷ and the earlier one of Nowicki *et al.*¹⁷ There was no indication of the previously reported 1.5 and 35 s half-lives.¹⁸ The mass separator measurement confirmed the mass assignment and the coincidences with x rays enabled the identification of Eu as the β -decay parent. The decay scheme developed in the present work has been given in a previous report which includes additional details of the experiment.⁶

C. $^{140}\text{Eu} \rightarrow ^{140}\text{Sm}$

Little was previously known about the beta decay of ^{140}Eu . A high-spin favoring reaction was reported¹⁹ to give a ^{140}Eu isomer which decayed with a half-life of $20(+15, -10)$ s giving several γ rays that were later recognized as belonging to an yrast cascade which was obtained in an in-beam experiment.²⁰ Recently, Redon *et al.*²¹ reported observing a 21 ± 3 s half-life for the 530.9-keV γ ray in an experiment where half-lives > 1 s could be detected. A low-spin favoring reaction was observed^{22,23} to give a ^{140}Eu isomer that decayed with a half-life of 1.5 s. Deslauriers²⁴ has given the half-life as 1.54 s for observed γ rays with energies 530.8, 459.6, and 1068.1 keV.

In order to continue the systematic consideration of the several light Sm isotopes we studied the decay of ^{140}Eu to ^{140}Sm with use of the UNISOR magnetic isotope separator. A target of natural Mo was bombarded by a beam of 220-MeV ^{48}Ti ions. An earlier UNISOR experiment had failed to detect the 20-s half-life; again, in the present experiment, there was no indication of a high-spin 20-s isomer, when collecting and counting for 35 s intervals. When collecting and counting for 5 s intervals, we did observe the 530.9-keV γ ray from the ^{140}Sm first-excited level decaying with a half-life of 1.5 ± 0.3 s, as shown in Fig. 3, in agreement with Refs. 22-24. Gamma rays with energies of 459.9 and 1067.4

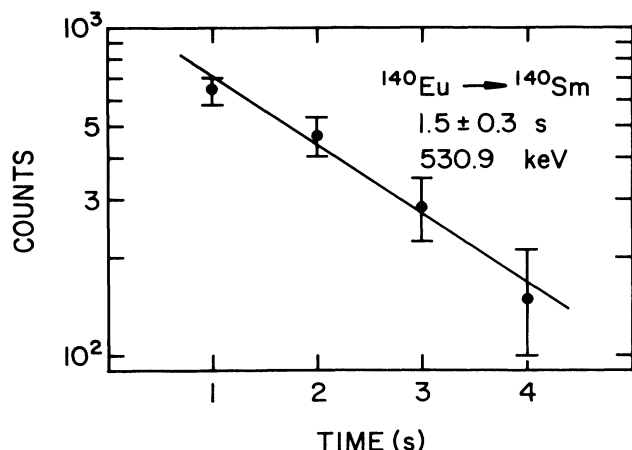


FIG. 3. The decay of the 530.9-keV γ ray due to the beta decay of ^{140}Eu .

keV were found to be in coincidence with the 530.9-keV γ ray. A very low-intensity 607.5-keV γ ray is tentatively assigned to the 1598.3- to 990.5-keV transition. A partial decay scheme is shown in Fig. 4. The tentative identification of the 990.5 and 1598.3 keV levels as the 2^+ and 3^+ members of the quasigamma band is consistent with the systematics of this region.

IV. DEFORMED WOODS-SAXON MODEL CALCULATIONS

A. Method of calculation

The potential energy of β_2 , γ , and β_4 deformation was calculated by the Strutinsky method.²⁵ The triaxially deformed Woods-Saxon single-particle potential developed by the Warsaw group⁸ was used with a “universal” set of parameters²⁶ that has previously been widely employed from the mass ≈ 80 region to the actinides. The poten-

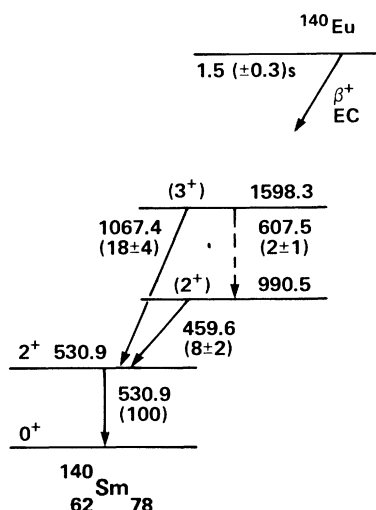


FIG. 4. Partial level diagram for ^{140}Sm . The energies are in keV and the relative intensities are given in the parentheses.

tial energy was calculated on a square lattice in the quadrupole deformation plane with a lattice constant 0.05, and at steps of 0.04 in β_4 .

Spectroscopic properties were subsequently calculated at the interpolated minima in β_2 , γ , and β_4 . The quadrupole transition moments were obtained, somewhat crudely, by considering axial β_2 and β_4 deformation only and assuming a homogeneous charge distribution with the radius parameter $r_0 = 1.18$ fm. The $B(E2; 2^+ \rightarrow 0^+)$ reduced transition rate was then obtained from the standard rotational model formula.²⁷ The rotational moments of inertia with respect to the three principal axes were obtained by solving the cranked Woods-Saxon-Bogolyubov equations²⁸ at a rotational frequency of $\hbar\omega = 100$ keV around each of the axes. The self-consistent pairing gap parameter, but not the shape, was redetermined for the rotating solution. The three moments of inertia were then obtained as

$$\mathcal{J}_{1,2,3} = I_{1,2,3} / \omega, \quad (1)$$

where $\langle I_\kappa \rangle$ is the projection of the angular momentum of the nucleons along the cranking axis. The 2^+ excitation energy is

$$E_{1\text{-axial}}(2_1^+) = (2 + \frac{1}{2})^2 \hbar^2 / 2\mathcal{J}_{\text{max}}, \quad (2)$$

in a semiclassical approximation of rotation around the axis with the largest moment of inertia, \mathcal{J}_{max} . For triaxial shapes, a different value of $E(2_1^+)$ was obtained by solving the quantum mechanical triaxial rotor Hamiltonian,

$$\hat{H}_{3\text{-axial}} = \hbar^2 / 2 (\hat{I}_1^2 / \mathcal{J}_1 + \hat{I}_2^2 / \mathcal{J}_2 + \hat{I}_3^2 / \mathcal{J}_3). \quad (3)$$

The calculated moments of inertia are very sensitive to the Bardeen-Cooper-Schrieffer (BCS) pairing matrix element, G . A recent empirical study of Jensen *et al.*²⁹ has shown that the average dependence of pairing on the neutron-proton asymmetry $N - Z$ is stronger than was believed previously. On the basis of measured odd-even mass differences, Δ_{oe} , including recent data on nuclei far from stability, Jensen *et al.* propose a formula for the average N and Z dependence of the odd-even mass differences, $\bar{\Delta}_{oe}(N, Z)$. In order to extrapolate into the neutron-deficient Sm region, we calculate G values for each nucleus at each deformation by the average gap method,³⁰ taking the average gap $\bar{\Delta}$ to be

$$\bar{\Delta} = 0.9 \bar{\Delta}_{oe}(N, Z). \quad (4)$$

The factor of 0.9 in Eq. (4) is chosen *ad hoc* so as to obtain agreement between Eq. (2) and experimental 2^+ energies for well-deformed nuclei both above and below $N = 82$. With this factor, the theoretical and experimental values are 82 versus 86 keV in ^{154}Sm and 163 versus 163 keV in ^{134}Sm . The same factor 0.9 was previously found to be appropriate in combination with the modified oscillator single-particle potential.⁶ The potential-energy surfaces are much less sensitive to the pairing than the moments of inertia, and were calculated (before the factor 0.9 could be determined at the resulting minima) with a standard prescription³¹ for G and approximate particle number projection before variation.³²

TABLE I. Ground-state deformations, β_2 , β_4 , and γ , in the potential-energy surfaces calculated by the Woods-Saxon-Strutinsky method. V_{om} is the potential-energy difference between the minimum under constraint of oblate shape and the absolute minimum.

Z	N	β_2	β_4	γ	V_{om} (keV)	Z	N	β_2	β_4	γ	V_{om} (keV)	
^{52}Te	60	0.135	0.021	0	360	^{58}Ce	70	0.260	0.016	0	1381	
	62	0.135	0.017	0	190		72	0.232	0.005	0	990	
	64	0.128	0.014	2	44		74	0.194	-0.004	5	719	
	66	0.120	0	60			76	0.165	-0.008	17	475	
	68	0.117	0	60			78	0.117	-0.005	2	265	
	70	0.106	0	60			80	0.021	0	13		
	72	0.087	0	60			^{60}Nd	60	0.313	0.047	0	3606
	74	0	0					62	0.317	0.040	0	3617
	76	0	0					64	0.315	0.033	0	3445
	78	0	0					66	0.311	0.027	0	3115
80	0	0			68	0.307		0.021	0	2653		
^{54}Xe	60	0.190	0.033	0	1158	70		0.299	0.015	0	2055	
	62	0.199	0.030	0	991	72		0.284	0.005	0	1429	
	64	0.202	0.027	0	796	74		0.229	-0.006	8	852	
	66	0.203	0.024	0	637	76	0.190	-0.012	20	579		
	68	0.197	0.021	0	451	78	0.132	-0.009	1	243		
	70	0.181	0.015	0	299	80	0.039	-0.001	2	17		
	72	0.160	0.009	7	201	^{62}Sm	62	0.327	0.034	0	3910	
	74	0.133	0.003	11	132		64	0.324	0.026	0	3949	
	76	0.098	0.001	9	19		66	0.319	0.019	0	3815	
	78	0	0				68	0.316	0.014	0	3567	
80	0	0			70		0.311	0.009	0	3121		
^{56}Ba	60	0.239	0.040	0	1691		72	0.302	0	0	2544	
	62	0.251	0.037	0	1619		74	0.283	-0.009	0	1897	
	64	0.250	0.032	0	1487		76	0.214	-0.015	23	1176	
	66	0.246	0.027	0	1316	78	0.165	-0.009	25	622		
	68	0.238	0.022	0	1087	80	0.033	-0.001	8	164		
	70	0.221	0.015	0	830	^{64}Gd	70	0.310	0	0	2818	
	72	0.196	0.007	1	641		72	0.301	-0.007	0	2129	
	74	0.170	0.001	9	478		74	0.283	-0.015	0	1374	
	76	0.137	0.001	2	296		76	0.236	-0.019	20	666	
	78	0.093	0	3	136	78	0.182	-0.008	31	53		
80	0.007	0	60		80	0.029	-0.001	14	11			
^{58}Ce	60	0.289	0.050	0	2604	^{66}Dy	74	0.282	-0.019	0	1463	
	62	0.297	0.045	0	2605		76	0.253	-0.022	17	618	
	64	0.294	0.038	0	2454		78	0.183	-0.001	60		
	66	0.288	0.031	0	2177		80	0.042	-0.001	60		
	68	0.279	0.025	0	1804							

B. Results of calculations

The equilibrium deformations obtained with the present Woods-Saxon model (WS) are given in Table I for all the nuclei considered in the $50 < Z, N < 82$ region. The potential-energy difference, V_{om} , between the minimum under constraint of oblate deformation and the absolute minimum is also tabulated. Potential-energy surfaces for $^{134-142}\text{Sm}$ in the β, γ plane, minimized with respect to β_4 , are plotted in Fig. 5. The transition from well-deformed prolate shape in $^{134}\text{Sm}_{72}$ to near-spherical shape in $^{142}\text{Sm}_{80}$ is seen to proceed via triaxial shapes in $^{138,140}\text{Sm}_{76,78}$, in agreement with the modified oscillator³ (MO) and Skyrme III Hartree-Fock^{4,21,33} (SIII) calculations mentioned above. In the following, first we provide further spectroscopic evidence for a triaxial interpretation of the transitional Sm isotopes. Next we focus on *differences* between WS, MO,

SIII, and folded Yukawa model^{34,35} (FY) potential-energy surfaces, and possible experimental tests.

The WS calculated rotational moments of inertia for $^{130-140}\text{Sm}$, and the associated pairing gap parameters at $\omega=0$, are listed in Table II. The corresponding energy spectra from Eqs. (2) and (3) are compared with the data in Figs. 6 and 7. First let us inspect the lowest 2^+ state (Fig. 6). For axial shapes, its energy should be given by the cranking formulas (1) and (2) for 1-axial rotation. In the light Sm isotopes this formula, applied to the calculated equilibrium shapes of the WS model, gives a variation of the 2^+ energy which is much smaller than the variation observed in experiment (lower dashed curve versus filled circles in Fig. 6). However, the onset of triaxiality for larger N can account for the observed variation of the 2^+ energy within the framework of the triaxial rotor model. When the cranking formula (1) is applied to each of the three principal axes, and the 2^+

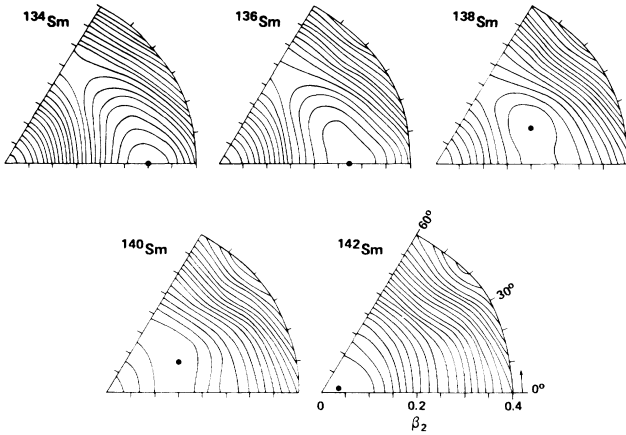


FIG. 5. Potential-energy surfaces in the β, γ quadrupole deformation plane for $^{134-142}\text{Sm}$ from the Woods-Saxon-Strutinsky calculations. The potential energy at each point is minimized with respect to β_4 . The contour line separation is 250 keV.

energy is obtained by solving the resulting triaxial rotor Hamiltonian (3), the results for $N = 76$ and 78 are as indicated by the upper dashed curve in Fig. 6. The lower dashed curve in Fig. 6 should be relevant for $N \leq 72$.

The solution of the triaxial rotor Hamiltonian (3) also reproduces the energies of the 2_2^+ and 3_1^+ members of the γ band quite well for $N = 76$ and 78 (Fig. 7). The states of spin 4 and up are systematically lower in experiment than in theory, however, reflecting the variable moment of inertia effect. This effect is generally attributed to changes of the shape and pair fields at higher spins which were not taken into account in the theoretical spectra of Fig. 7. Nevertheless, the experimental 4_2^+ γ -band member is observed to lie well above the 3_1^+ level in ^{138}Sm . The solution of the Bohr Hamiltonian in the SIII calculated potential-energy surface leads to a much smaller spacing between the 3_1^+ and 4_2^+ levels,³³ which suggests that the role of quadrupole shape vibrations is exaggerated in this approach and that the triaxial rotor description is unusually pertinent for ^{138}Sm .

The present WS potential-energy surfaces differ from the MO and SIII surfaces in that prolate shapes are systematically more favored relative to oblate shapes by the

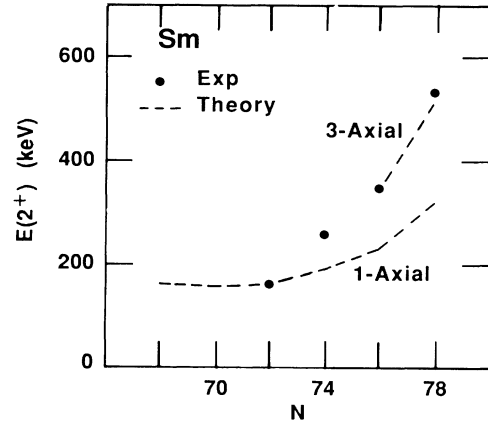


FIG. 6. First 2^+ energies of the light Sm isotopes calculated from the Woods-Saxon deformed shell model (dashed lines) are compared with experimental data (solid circles). The calculated values marked “1-axial” are from a semiclassical treatment of the rotation, while those marked “3-axial” were obtained for the triaxial cases by quantal triaxial rotations. In the $N \leq 72$ isotopes, which have stable axial symmetry, the “1-axial” curve also applies for quantal rotations.

WS model. Comparing V_{om} in Table I with the MO results in Ref. 3, this is found to be the case not only for the light Sm isotopes but also for all particle-stable deformed nuclei in the $50 < Z, N < 82$ region. This aspect of the potential-energy surfaces could be tested experimentally by observing the band structure at high spins, since the rotational alignment of certain single-particle orbits requires a transition to oblate shape.³⁶

The β_2 deformation in the shape transitional light Sm isotopes exhibits considerable model sensitivity. The 2^+ energies are too crude a measure of β_2 deformation to test these model differences.⁶ A better measure is the $B(E2; 2 \rightarrow 0)$ transition rate, and several experiments have been made.^{11,16,37,38} Unfortunately they are not yet conclusive since widely different results have been obtained for $^{136}\text{Sm}_{74}$ (Fig. 8). The intrinsic quadrupole moment makes a sharp jump between $N = 72$ and 74 in the FY and SIII models, as in the Daresbury data³⁸ indicated by squares in Fig. 8. It varies smoothly with N in the MO model. It varies rather smoothly in the present WS

TABLE II. Properties of $^{130-140}\text{Sm}$ calculated by the Woods-Saxon-Bogolyubov-Strutinsky deformed shell model approach described in the text. $\mathcal{J}_{1,2,3}$ are the rotational moments of inertia around the three principal axes, Δ_n and Δ_p are the neutron and proton pairing gap parameters, and Q_0 is the intrinsic quadrupole moment.

N	\mathcal{J}_1	\mathcal{J}_2 ($\hbar^2 \text{MeV}^{-1}$)	\mathcal{J}_3	Δ_n (MeV)	Δ_p (MeV)	Q_0 (b)
68	19.65	19.65		1.14	1.15	5.94
70	19.90	19.90		1.10	1.15	5.88
72	19.17	19.17		1.12	1.18	5.70
74	16.45	16.45		1.16	1.21	5.30
76	13.56	6.30	2.73	0.95	1.31	3.95
78	9.86	3.86	2.33	0.84	1.38	3.06

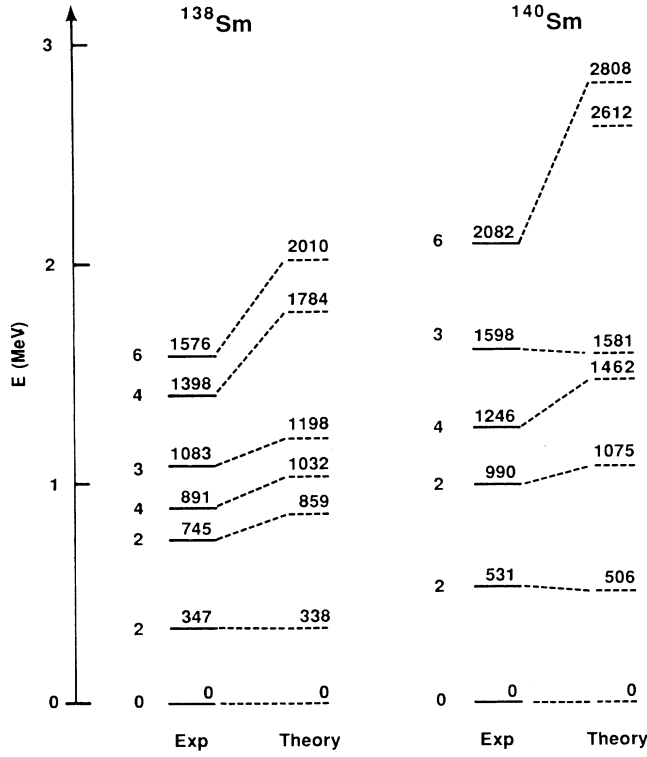


FIG. 7. Triaxial rotor model spectra for $^{138,140}\text{Sm}$, with moment of inertia parameters obtained from the Woods-Saxon deformed shell model at $I=0$, are compared with experiment. Note the agreement for the $I \leq 3$ states, while the higher spin states increasingly exhibit a variable moment of inertia effect.

model, with the largest jump between $N=74$ and 76 , as shown by the solid curve in Fig. 8. The WS is in agreement with the Padova data^{16,37} indicated by filled circles. For the nucleus $^{138}\text{Sm}_{76}$, central to the arguments above regarding triaxiality, there is good compatibility between the WS equilibrium deformation and two independent $B(E2)$ measurements.^{11,37}

V. INTERACTING BOSON MODEL CALCULATIONS

One interesting aspect of the proton-neutron version of the interacting boson model (IBM-2) is the possibility of making detailed predictions based on parameters deduced from a set of well-studied nuclei. We test this predictive power by applying the IBM-2 to our Sm data

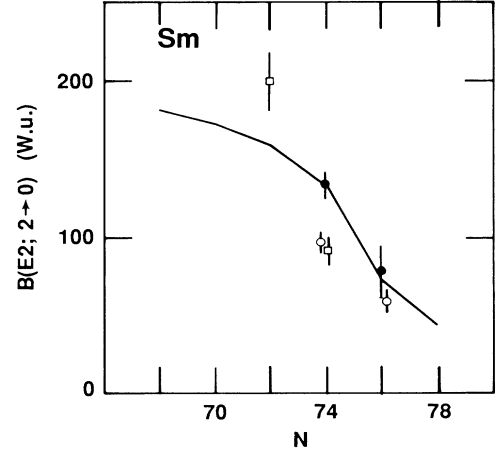


FIG. 8. Reduced $E2$ transition rates from the first 2^+ state to the ground state of the light Sm isotopes. The solid curve was calculated from the Woods-Saxon-Strutinsky equilibrium shapes with a charge radius parameter $r_0=1.18$ fm. The solid circles represent the experimental data of the Padova group (Refs. 16 and 37), the open circles those of Makishima *et al.* (Ref. 11), and the open squares those of Wadsworth *et al.* (Ref. 38).

without any parameter fitting.

The IBM-2 Hamiltonian is given by

$$H = \epsilon(n_{d_\pi} + n_{d_\nu}) + \kappa Q_\pi Q_\nu + V_{\pi\pi} + V_{\nu\nu} + M_{\pi\nu} \quad (5)$$

with

$$Q_\rho = d_\rho^\dagger s_\rho + s_\rho^\dagger \tilde{d}_\rho + \chi_\rho (d_\rho^\dagger \tilde{d}_\rho)^{(2)}, \quad \rho = \pi, \nu \quad (6)$$

where Q_π (Q_ν) is the proton (neutron) boson quadrupole operator. $V_{\pi\pi}$ ($V_{\nu\nu}$) is a residual two-body interaction between proton (neutron) bosons, $M_{\pi\nu}$ is the Majorana term, and n_{d_π} (n_{d_ν}) counts the number of proton (neutron) d bosons. The microscopic calculations of Ref. 39 predict the dependence of the parameters on the number of proton and neutron bosons, N_π and N_ν , respectively. Guided by those results, we assume as in Ref. 10 that the parameters C_L^π (in the residual boson-boson interaction $V_{\pi\pi}$) and χ_π depend only on N_π , and similarly C_L^ν and χ_ν depend only on N_ν . Furthermore, we adopt the result¹⁰ that ϵ and κ seem to depend only on N_ν in this region. Under these assumptions, a first parameter set was obtained by taking χ_π and C_L^π from previous⁹ Sm calculations for $N > 82$, and the remaining parameters

TABLE III. Parameters (Refs. 9–11) of IBM-2 used in the present work for $^{136,138,140}\text{Sm}$. For both sets: $C_{L=0}^\pi=0.0$, $C_{L=2}^\pi=0.05$, $C_{L=4}^\pi=0.0$ ($N_\pi=6$), $C_{L=0}^\nu=0.3$, $C_{L=2}^\nu=0.0$ ($N_\nu=4$), and $C_{L=2}^\nu=0.1$ ($N_\nu=2,3$), $C_{L=4}^\nu=0.0$, and in the Majorana term FS=0.120 and FK=0.210. FS and FK are defined in Ref. 9, and are equivalent to $\xi_1=-0.09$, $\xi_2=0.120$, and $\xi_3=\xi_1$.

	Parameter set 1				Parameter set 2			
	κ	ϵ	χ_ν	χ_π	κ	ϵ	χ_ν	χ_π
$^{136}_{62}\text{Sm}_{74}$	-0.17	0.70	0.30	-1.3	-0.15	0.70	0.40	-1.00
$^{138}_{62}\text{Sm}_{76}$	-0.19	0.80	0.50	-1.3	-0.15	0.78	0.60	-1.00
$^{140}_{62}\text{Sm}_{78}$	-0.21	0.90	0.90	-1.3	-0.15	0.86	0.80	-1.00

EXPERIMENT	IBA-2 (PARAMETER SET 1)	IBA-1 (PARAMETER SET 2)
	4 ⁺ 1704	
6 ⁺ 1225	3 ⁺ 1568	4 ⁺ 1434
	2 ⁺ 1188	3 ⁺ 1370
	3 ⁺ 1173	6 ⁺ 1265
	6 ⁺ 1156	2 ⁺ 871
	2 ⁺ 714	4 ⁺ 682
4 ⁺ 689	4 ⁺ 584	
2 ⁺ 256	2 ⁺ 193	2 ⁺ 255
0 ⁺	0 ⁺	0 ⁺
¹³⁶ Sm 62 74	¹³⁶ Sm 62 74	¹³⁶ Sm 62 74
6 ⁺ 1577	4 ⁺ 1720	4 ⁺ 1574
	3 ⁺ 1654	6 ⁺ 1587
	6 ⁺ 1492	3 ⁺ 1546
	3 ⁺ 1084	2 ⁺ 1056
4 ⁺ 891	2 ⁺ 1056	2 ⁺ 911
	4 ⁺ 807	4 ⁺ 904
	2 ⁺ 746	
2 ⁺ 347	2 ⁺ 303	2 ⁺ 370
0 ⁺	0 ⁺	0 ⁺
¹³⁸ Sm 62 76	¹³⁸ Sm 62 76	¹³⁸ Sm 62 76
6 ⁺ 2082	6 ⁺ 2050	6 ⁺ 1992
	4 ⁺ 1908	3 ⁺ 1857
	3 ⁺ 1598	
4 ⁺ 1246	4 ⁺ 1189	4 ⁺ 1185
	2 ⁺ 1098	2 ⁺ 1140
	2 ⁺ 990	
2 ⁺ 531	2 ⁺ 493	2 ⁺ 511
0 ⁺	0 ⁺	0 ⁺
¹⁴⁰ Sm 62 78	¹⁴⁰ Sm 62 78	¹⁴⁰ Sm 62 78

FIG. 9. The experimental spectra, the IBM-2 calculated spectra with parameter set 1 of Table III, and the calculated spectra with parameter set 2 are shown for ^{136,138,140}Sm. Note that these parameter sets reproduce neither the low energy of the γ band head, nor the wide spacing between the 3⁺ and 4⁺ members of the γ band of ¹³⁸Sm.

from previous¹⁰ calculations for the Xe-Ba-Ce region with $N < 82$. Also, a second parameter set was chosen by taking ϵ , κ , χ_{π} , and χ_{ν} from Ref. 11, where they were fitted to the ground bands in ^{136,138}Sm, and all other parameters taken as above. (Makishima *et al.*¹¹ do not provide a complete parameter set in their paper. It may

be remarked that we reproduce their energy spectra with the usual $Z = 50$ core, $N_{\pi} = 6$, and not with the $Z = 64$ core, $N_{\pi} = 1$, which they claim to have used.) Since the yrast energies were fitted, only the γ band energies can be considered as predictions for the second parameter set. The two parameter sets are given in Table III, and the calculated spectra are compared with the data in Fig. 9.

The calculations based on the first parameter set are seen to underestimate the energy of the 2₁⁺ state systematically and to compress the ground band slightly compared to the data. For the γ band, both the energy of the 2₂⁺ band head and the odd-even staggering in the band are overestimated, although the 4₂⁺-2₂⁺ energy spacing is approximately correct. Using the second parameter set, the predicted energy of the 2₂⁺ state is improved, but is still too high, and the staggering in the γ band remains far too large. In summary, the accuracy of the IBM predictions is much worse for the gamma band than for the ground band in these nuclei.

VI. CONCLUSIONS

The yrast bands of the ^{136,138,140}Sm isotopes recently became known through in-beam spectroscopy, and the γ bands have now been observed through beta decay studies. The γ bands provide experimental information with bearing on one of the structural differences between the $N < 82$ and $N > 82$ shape transitional isotopes. Deformed shell model and Hartree-Fock calculations uniformly predict triaxial intrinsic shapes specifically for the $N < 82$ transitional Sm isotopes, and this is supported by the observed spectra. The γ bands come low in energy, lower than expected from extrapolations of IBM-2 that are based on $N > 82$ Sm nuclei, on $N < 82$ and $Z < 62$ nuclei, and on the yrast levels of $N < 82$ Sm nuclei. Also, both IBM-2 and the Bohr Hamiltonian lead to a larger energy staggering of odd and even spin states than is observed experimentally, suggesting that the collective wave functions should be more localized in the γ degree of freedom. The triaxial rotor model, with parameters that are not fitted but derived from the Woods-Saxon version of the deformed shell model studied in this paper, reproduces the observed spectra quite well if allowance is made for a variable moment of inertia effect in the higher spin states. Furthermore, the large change in the yrast 2⁺ energy between ¹³⁴Sm and ¹⁴⁰Sm can be understood within the framework of the present deformed shell model by taking into account triaxial rotation of the heavier isotopes, which tends to increase the 2⁺ energy.

Support for this work was provided by the U.S. Department of Energy under Contract Nos. DE-AC05-76OR00033, DE-AS05-76ER0-3346, DE-AC05-84OR21400, and DE-FG05-84ER40159.

- *Present address: Institute of Physics, Warsaw Institute of Technology, PL-00-662 Warsaw, Poland.
- [†]Present address: Department of Physics, Tennessee Technological University, Cookeville, TN 38505.
- ¹R. K. Sheline, *Rev. Mod. Phys.* **32**, 1 (1960).
- ²C. J. Lister, B. J. Varley, R. Moscrop, W. Gelletly, P. J. Nolan, D. J. G. Love, P. J. Bishop, A. Kirwan, D. J. Thornley, L. Ying, R. Wadsworth, J. M. O'Donnell, H. G. Price, and A. H. Nelson, *Phys. Rev. Lett.* **55**, 810 (1985).
- ³I. Ragnarsson, A. Sobiczewski, R. K. Sheline, S. E. Larsson, and B. Nerlo-Pomorska, *Nucl. Phys.* **A233**, 329 (1974).
- ⁴N. Redon, J. Meyer, M. Meyer, P. Quentin, M. S. Weiss, P. Bonche, H. Flocard, and P.-H. Heenen, *Phys. Lett.* **181B**, 223 (1986).
- ⁵R. L. Mlekodaj, G. A. Leander, M. O. Kortelahti, B. D. Kern, R. A. Braga, C. P. Perez, and B. E. Gnade, *Bull. Am. Phys. Soc.* **31**, 836 (1986).
- ⁶R. L. Mlekodaj, G. A. Leander, R. A. Braga, B. D. Kern, K. S. Toth, and B. E. Gnade, *Nuclei Off the Line of Stability*, ACS Symposium Series No. 324, edited by R. A. Meyer and D. S. Brenner (American Chemical Society, Washington, D.C., 1986), p. 502.
- ⁷A. Charvet, T. Ollivier, R. Beraud, R. Duffait, A. Emsallem, N. Idrissi, J. Genevey, and A. Gizon, *Z. Phys. A* **321**, 697 (1985).
- ⁸W. Nazarewicz, J. Dudek, R. Bengtsson, T. Bengtsson, and I. Ragnarsson, *Nucl. Phys.* **A435**, 397 (1985).
- ⁹O. Scholten, Ph.D. thesis, University of Groningen, 1980; O. Scholten, KVI-253 (1979).
- ¹⁰G. Puddu, O. Scholten, and T. Otsuka, *Nucl. Phys.* **A348**, 109 (1980).
- ¹¹A. Makishima, M. Adachi, H. Taketani, and M. Ishii, *Phys. Rev. C* **34**, 576 (1986).
- ¹²E. H. Spejewski, R. L. Mlekodaj, and H. K. Carter, *Nucl. Instrum. Methods* **186**, 71 (1981).
- ¹³D. M. Moltz, *Nucl. Instrum. Methods* **186**, 135 (1981).
- ¹⁴R. L. Mlekodaj, E. F. Zganjar, and J. D. Cole, *Nucl. Instrum. Methods* **186**, 239 (1981).
- ¹⁵B. D. Kern, R. L. Mlekodaj, M. O. Kortelahti, E. F. Zganjar, R. A. Braga, R. W. Fink, and C. P. Perez (unpublished).
- ¹⁶S. Lunardi, F. Scarlassara, F. Soramel, S. Beghini, M. Morando, C. Signorini, W. Meczynski, W. Starzecki, G. Fortuna, and A. M. Stefanini, *Z. Phys. A* **321**, 177 (1985).
- ¹⁷M. Nowicki, D. D. Bogdanov, A. A. Demyanov, and Z. Stachura, *Acta Phys. Pol.* **3B**, 879 (1982).
- ¹⁸D. D. Bogdanov, A. V. Demyanov, V. A. Karnaukhov, L. A. Petrov, A. Plohocki, V. G. Subbotin, and J. Voboril, *Nucl. Phys.* **A275**, 229 (1977).
- ¹⁹D. Habs, H. Klewe-Nebenius, R. Loehken, S. Goering, J. van Klinken, H. Rebel, and G. Schatz, *Z. Phys. A* **250**, 179 (1972).
- ²⁰M. A. J. Mariscotti, H. Beuscher, W. F. Davidson, R. M. Lieder, A. Neskakis, and H. M. Jaeger, *Z. Phys. A* **279**, 169 (1976).
- ²¹N. Redon, T. Ollivier, R. Beraud, A. Charvet, R. Duffait, A. Emsallem, J. Honkanen, M. Meyer, J. Genevey, A. Gizon, and N. Idrissi, *Z. Phys. A* **325**, 127 (1986).
- ²²L. Westgaard and the ISOLDE Collaboration, *Bull. Am. Phys. Soc.* **17**, 907 (1972).
- ²³L. Westgaard, P. G. Hansen, B. Jonson, H. L. Ravn, and S. Sundell, in *Proceedings of the International Conference on Nuclear Physics*, Munich, 1973, Vol. 1, p. 696.
- ²⁴J. Deslauriers, Ph.D. thesis, McGill University, 1979.
- ²⁵V. M. Strutinsky, *Nucl. Phys.* **A95**, 420 (1967); **A122**, 1 (1968).
- ²⁶J. Dudek, Z. Szymański, and T. Werner, *Phys. Rev. C* **23**, 920 (1981).
- ²⁷A. Bohr and B. R. Mottelson, *Nuclear Structure* (Benjamin, New York, 1975), Vol. 2.
- ²⁸S. Cwiok, W. Nazarewicz, J. Dudek, J. Skalski, and Z. Szymański, *Nucl. Phys.* **A333**, 139 (1980).
- ²⁹A. S. Jensen, P. G. Hansen, and B. Jonson, *Nucl. Phys.* **A431**, 393 (1984).
- ³⁰M. Brack, J. Damgaard, A. S. Jensen, H. C. Pauli, V. M. Strutinsky, and C. Y. Wong, *Rev. Mod. Phys.* **44**, 320 (1972).
- ³¹J. Dudek, A. Majhofer, and J. Skalski, *J. Phys. G* **6**, 447 (1980).
- ³²H. J. Lipkin, *Ann. Phys. (N.Y.)* **9**, 272 (1980).
- ³³Ph. Quentin, private communication.
- ³⁴P. Möller and J. R. Nix, *At. Data Nucl. Data Tables* **26**, 165 (1981).
- ³⁵G. Leander and P. Möller, *Phys. Lett.* **110B**, 17 (1982).
- ³⁶Y. S. Chen, S. Frauendorf, and G. A. Leander, *Phys. Rev. C* **28**, 2437 (1983).
- ³⁷F. Soramel, S. Lunardi, W. Meczynski, and M. Morando, in *Weak and Electromagnetic Interactions in Nuclei*, edited by H. V. Klapdor (Springer, Berlin, 1986), p. 127.
- ³⁸R. Wadsworth, J. M. O'Donnell, D. L. Watson, P. J. Nolan, P. J. Bishop, D. J. Thornley, A. Kirwan, and D. J. G. Love, *J. Phys. G* **13**, 205 (1987).
- ³⁹T. Otsuka, A. Arima, and F. Iachello, *Nucl. Phys.* **A309**, 1 (1978).